

Kinetics of Hydrogen Reduction of Ferrous Oxide in a Batch Fluidized Bed: Effects of Mass Velocity and Pressure

W. D. AHNER and JEROME FEINMAN

United States Steel Corporation, Monroeville, Pennsylvania

The kinetics of reduction of ferrous oxide with hydrogen were studied in a 1½-in. diameter isothermal batch fluidized reactor. The effects of mass velocity and pressure on the reduction path were investigated over the ranges 5.3 to 19.2 moles/sq.ft.hr. and 1.3 to 5.4 atm. at 1,000° and 1,300°F. The results are correlated by means of instantaneous oxygen balances on the assumptions that there are no oxygen concentration gradients in the solid phase, that the distribution of residence times for the gas flow is represented closely by assuming complete mixing, and that the reduction rate is controlled at the oxide-metal interface. The rate of reduction increased with increasing pressure and mass velocity. An excellent correlation was obtained for the program at 1,000°F. At 1,300°F. sintering and grain growth of the product layer complicated the reduction process, and a correlation was not obtained. Application of the results to the design of commercial fluidized-reduction processes is discussed qualitatively.

In a previous study (1) an isothermal batch fluidized reactor was used to investigate the effects of particle size and temperature on the kinetics of hydrogen reduction of ferrous oxide made from Venezuelan ore fines. This study showed that within the range of particle sizes suitable for fluidization reduction rate is independent of particle size. This result is explained on the basis that the particles of ferrous oxide made from Venezuelan ore are extremely porous, precluding the topochemical reduction mechanism found when dense nonporous particles are reduced. The individual grains making up the particles are much smaller than the particles themselves, and accessibility of grains to the reactant gas must be nearly independent of their location in the particle because micrographic examination of partially reduced particles mounted in plastic indicated that there were no oxygen gradients in the particles. In addition chemical analyses of sized fractions of partially reduced particles from continuous pilot-plant studies with minus 10-mesh ore showed that the large particles were at about the same state of reduction as the small ones. The study of the effect of temperature showed that above about 1,030°F. the reduction rate decreases sharply as reduction proceeds, becoming very low above 80% reduction. Below about 1,030°F. however the rate does not fall off until reduction is practically complete. This result is explained as follows. Up to 1,030°F. the iron product is very porous and offers little resistance to diffusion of the reaction gases. Above 1,030°F. grain growth and sintering cause the iron product layer to lose its original porosity, thus hindering the free exchange of the reaction gases by diffusion. In effect residual oxide sources become surrounded by a relatively impermeable barrier of iron product.

Other factors important in the design and development of large-scale fluidized reduction processes that are amenable to study in laboratory-scale fluidized beds are gas composition, gas mass velocity, and gas pressure. Because the fluidized reduction processes under investigation by

the U.S. Steel Applied Research Laboratory at the time of this work (1, 2) were based on high-purity hydrogen, this laboratory investigation was limited to studying the effects of gas mass velocity and gas pressure on reduction kinetics.

EQUIPMENT AND EXPERIMENTAL PROCEDURE

Figure 1 is a schematic diagram of the equipment; Figure 2 shows details of the gas preheat and reduction vessels. A complete description of the system and the experimental procedure is presented elsewhere (1). In this work the reactor was a 1½-in. ID stainless steel cylinder instead of the 2-in. cylinder used previously.

A brief summary of the experimental procedure follows. The system was heated to operating temperature, with nitrogen as the fluidizing gas, and gas balances were made to ensure that no leaks had developed during heat up. The nitrogen flow was replaced with pure hydrogen to start the run, and simultaneous wet-test-meter readings and time-of-run readings were recorded to give the cumulative off-gas volume vs. the time of

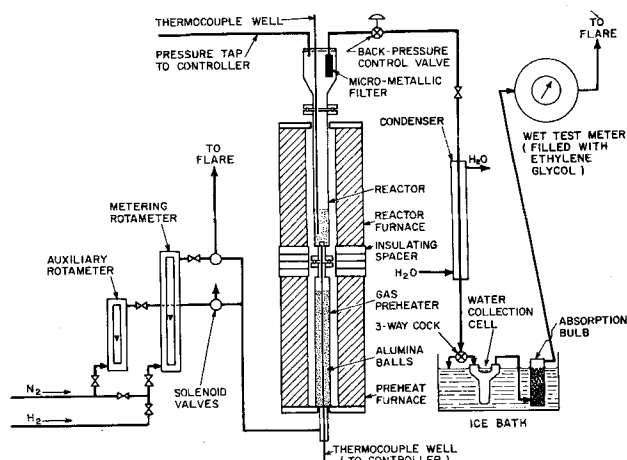


Fig. 1. Diagram of experimental apparatus.

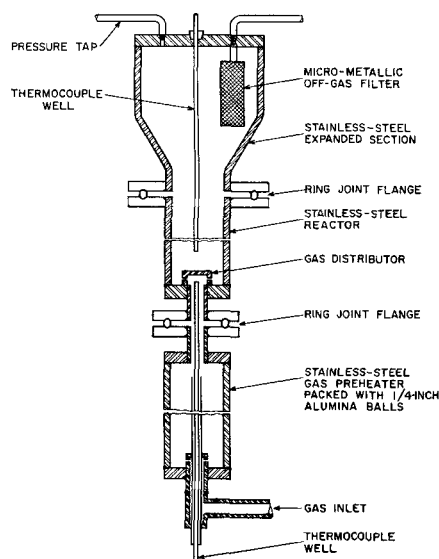


Fig. 2. Detail of gas-preheating and reduction system.

the run. The difference between the cumulative inlet and the cumulative outlet volume at any time represented the amount of water formed (that is oxygen removed from the iron oxide) from the start. It was thus possible to describe the course of the batch reduction completely (that is, percent reduction, or oxygen-to-iron ratio vs. time, or off-gas composition vs. time).

DESCRIPTION OF THE REACTION SYSTEM

Before the experimental program and the results obtained are discussed, it is instructive to consider a qualitative description of the reaction system. There are two interrelated phenomena that are pertinent to formulating an adequate picture, the reduction behavior of the particles comprising the bed and the flow distribution of the fluidizing gas, including gas-solid contact. Any mathematical analysis should be consistent with the knowledge about these factors.

The particles of ferrous oxide in the fluidized bed all have essentially the same degree of reduction at any given time. There are therefore no oxygen concentration gradients in the solid phase of the fluidized bed; the solid phase behaves as though it is perfectly mixed. In this study the gas distributor consisted of a small cap, with several symmetrically placed horizontal holes in its side wall, welded to the bottom of the reactor. At the bed entrance the gas sweeps radially outward across the bottom before being diverted by the reactor wall. The circulation pattern that is set up by the distributor consists of solids and associated gas moving downward centrally and upward peripherally. The height-to-diameter ratio for these runs was between 1.5 and 2.0. In such a shallow bed it is reasonable to expect that the circulation pattern imposed results in a distribution of residence times for the gas flow that is represented closely by assuming complete backmixing.

In view of this description of the mixing properties of the system the instantaneous oxygen balance for the bed at any time θ is

$$\text{Input rate} - \text{Output rate} = \text{Accumulation rate}$$

TABLE I. EXPERIMENTAL PROGRAM, RANGE OF VARIABLES

Temperature	1,000°F.	1,300°F.
Superficial gas velocity, ft/sec. (approximate)	1.3 1.6 1.9	1.2 1.5
π , atm.	1.3 to 3.7	1.7 to 5.4
G , lb. moles/hr. sq. ft.	6.9 to 19.2	5.3 to 16.9

or

$$Gy_o - Gy_\theta = V \frac{dS}{d\theta} \quad (1)$$

The rate at which a given particle loses oxygen $dS/d\theta$ was derived in reference 3 and is

$$\frac{dS}{d\theta} = -3 \left[\frac{Q}{r_o d_o} \right] \pi S^{2/3} \left(1 - y_n - \left[\frac{K+1}{K} \right] y \right) \quad (2)$$

This equation was derived on the basis that the reduction of the individual grains making up a porous oxide particle proceeds topochemically, that the rate of removal of oxygen is controlled at the oxide-metal interfaces of these grains, and that the rate of oxygen removal is proportional to the bulk stream hydrogen pressure in such a way that this rate decreases essentially linearly with increasing bulk stream water-vapor pressure and becomes zero at the equilibrium composition.

For this study $y_o = 0$ and $y_n = 0$. Equating (1) and (2) one gets

$$\left[\frac{Q}{r_o d_o} \right] = \frac{Gy_\theta}{3 V \pi \left(1 - \left[\frac{K+1}{K} \right] y_\theta \right) S^{2/3}} \quad (3)$$

When the data from an experiment are plotted as S vs. time, the instantaneous gas composition leaving the system (and in the bed by virtue of the assumption of perfect mixing) at any time θ can be calculated from Equation (2) and the measured slope $dS/d\theta$ at θ . The group

$\left[\frac{Q}{r_o d_o} \right]$ that represents the average kinetic and geometric properties of the oxide can then be calculated from

Equation (3). The rate function $\left[\frac{Q}{r_o d_o} \right]$ should be essentially constant over the course of a batch reduction. For

a given temperature $\left[\frac{Q}{r_o d_o} \right]$ should also be independent of pressure and of gas mass flow rate for relatively low pressures and mass flow rates (below the point at which the S vs. θ curve remains constant with increasing gas mass velocity). Where the S vs. θ curve no longer changes with increasing gas mass velocity, the product $\left[\frac{Q}{r_o d_o} \right] \pi$ should

be a constant for constant bed inventory V and gas mass velocity. There will obviously be a transition region between these two regimes for which neither condition holds. This experimental program was restricted to conditions in

which $\left[\frac{Q}{r_o d_o} \right]$ should be independent of pressure and gas mass velocity and to conditions in the transition region. This restriction was imposed because higher gas rates would require very high pressures to maintain dense phase fluidization.

EXPERIMENTAL PROGRAM AND RESULTS

The previous study showed that above about 1,030°F. the reduction rate decreases sharply as reduction proceeds, the rate being very low above 80% reduction, and that below 1,030°F. the rate does not fall off until reduction is essentially complete. It was therefore decided to study the effects of pressure and gas mass velocity at one representative temperature in each regime; the temperatures chosen were 1,000° and 1,300°F. Table I shows the ranges of superficial gas velocity, pressure, and gas mass velocity studied.

The ferrous oxide used was prepared by continuous reduction of Venezuelan ore with a mixture of hydrogen

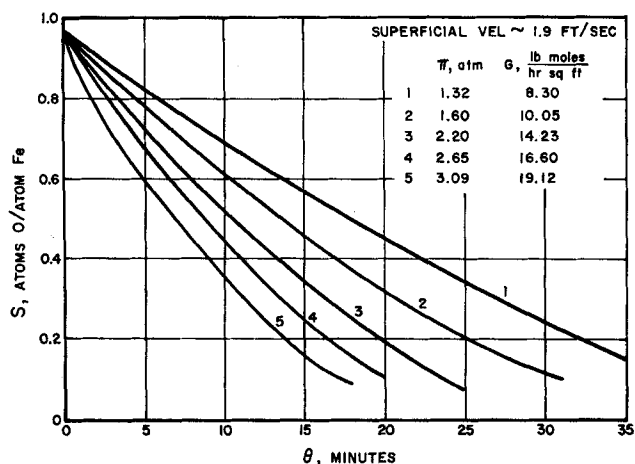


Fig. 3. Reduction paths for 1,000°F.

and water vapor in a 6-in. diameter fluidized-bed reactor. Table 2 shows the size distribution of the ferrous oxide (all plus 10-M and minus 100-M material was discarded). Table 3 presents the chemical analysis of the ferrous oxide. The bed inventory V was 0.565 lb. atoms Fe/sq.ft. for all runs.*

Figure 3 shows graphs of the reduction paths S vs. θ for the set of runs at 1.9 ft./sec. superficial gas velocity. It is evident that even for the highest pressure used the system is still far removed from that pressure above which the reduction curve would remain essentially constant. Clearly this condition also holds for the runs made at 1.6 and 1.3 ft./sec. Calculated values of the rate function $[Q/r_0 d_0]$ at various values of S during a typical run are presented in Table 4. The values of $[Q/r_0 d_0]$ are very nearly constant over the whole course of the batch reduction, in this case up to about 95% reduction. All the runs at 1,000°F. showed essentially this result; however for some of the runs the values of $[Q/r_0 d_0]$ deviate at high degrees of reduction (above about 90% reduction), where the values for S (and hence $S^{2/3}$) are very sensitive to any errors in the reduction-path data.

The average values of $[Q/r_0 d_0]$ calculated for all the 1,000°F. runs are plotted vs. G in Figure 4. With the exception of one high point at 1.9 ft./sec. all the values are within 7% of the curve drawn. $[Q/r_0 d_0]$ appears to decrease with increasing pressure and gas mass velocity, at least for pressures greater than about 2.5 atm. ($G > 11$

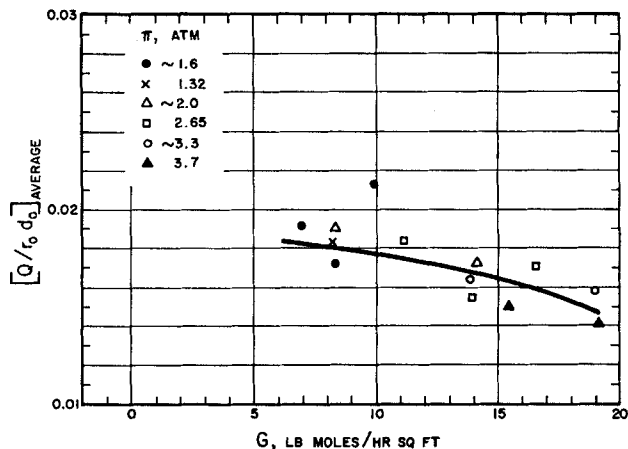


Fig. 4. $[Q/r_0 d_0]$ average vs. mass velocity G for 1,000°F.

lb. moles/sq. ft. hr.). For pressures below 2.5 atm. $[Q/r_0 d_0]$ appears to be relatively constant at an average value of 0.0180. These results are consistent with the results of a subsequent study of the effect of hydrogen pressure on the reduction of single dense magnetite pellets by McKewan (4). The hydrogen pressure range McKewan studied was 1 to 40 atm. over a temperature range of 630° to 932°F. At 932°F. the rate increased almost linearly with pressure up to about 2 atm. Above 2 atm. the rate increased asymptotically, becoming essentially constant above about 10 atm. In this present study it is the product $[Q/r_0 d_0]\pi$ that should be compared with the rate in McKewan's work. Thus for the pressure range where $[Q/r_0 d_0]$ is very nearly constant $[Q/r_0 d_0]\pi$ increases almost linearly with pressure. Above this pressure range $[Q/r_0 d_0]\pi$ will increase asymptotically to some constant value.

Program at 1,300°F.

Figure 5 shows graphs of the reduction paths S vs. θ for three values of G at 1.5 and 1.2 ft./sec. superficial velocity. Each path shows a fairly sharp decrease in oxygen removal rate between about 70 and 85% reduction ($S = 0.20$ to 0.45). Obviously the kinetics over the whole course of reduction cannot be described by means of a constant rate function, as was done for reduction at 1,000°F., because of the dependence of the reduction path on recrystallization and sintering of the product layer. The effect of sintering and grain growth can nevertheless

* Complete data for all the runs have been deposited as document 8008 with the American Documentation Institute, Photoduplication Service, Library of Congress, Washington 25, D. C., and may be obtained for \$1.25 for photoprints or 35-mm. microfilm.

TABLE 2. SIZE DISTRIBUTION OF FERROUS OXIDE

Screen size	% retained
20 M	15
35 M	26
65 M	36
80 M	14
100 M	9

TABLE 3. CHEMICAL ANALYSIS OF FERROUS OXIDE

Component	Weight fraction
Fe ^o	0.0461
FeO	0.8579
Fe ₂ O ₃	0.0795
Fe _{total}	0.7685
Gangue	0.0165

$$S_0 = 0.9766 \text{ atoms O/atom Fe}$$

TABLE 4. $[Q/r_0 d_0]$ vs. S FOR TYPICAL RUNS AT 1,000° AND 1,300°F.

Temperature, ° F.	1,000	1,300	
Run no.	259-15	259-41	
π , atm.	1.32	2.87	
G, lb. moles/hr. sq. ft.	8.30	12.08	
$K, \left(\frac{P_{H_2O}}{P_{H_2}} \right)_{eq}$	0.25 (refer-	0.433 (refer-	
	ence 5)	ence 6)	
S	$[Q/r_0 d_0]$	S	$[Q/r_0 d_0]$
0.883	0.0193	0.882	0.0672
0.770	0.0186	0.744	0.0552
0.663	0.0169	0.710	0.0481
0.566	0.0163	0.632	0.0396
0.449	0.0176	0.560	0.0343
0.339	0.0184	0.491	0.0218
0.259	0.0192	0.448	0.0103
0.153	0.0202	0.417	0.0068
0.075	0.0171		
<hr/>			
Average	0.0182		

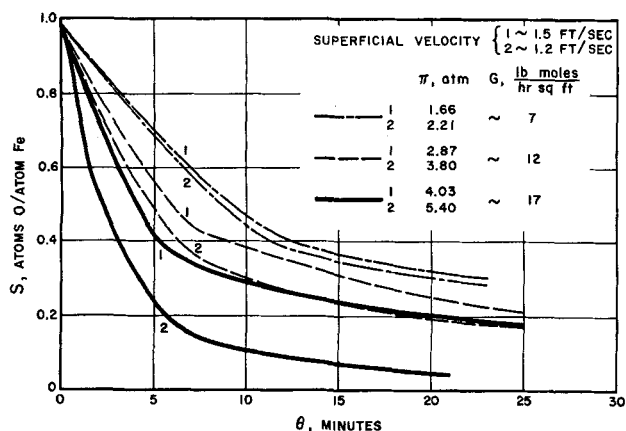


Fig. 5. Reduction paths showing effect of pressure and mass velocity at 1,300°F.

be observed semiquantitatively by calculating $[Q/r_0 d_0]$ for a typical run. Table 4 shows values of the rate function $[Q/r_0 d_0]$ at various values of S during one of the runs at 1.5 ft./sec. Apparently grain growth and sintering begin as soon as iron is formed, as evidenced by the fact that $[Q/r_0 d_0]$ decreases from the very start of reduction. For this run the rate became very slow below $S = 0.49$ corresponding to 67% reduction. It is also evident that a reduction model based on a simple diffusion mechanism cannot rationalize these results. In the first place a simple diffusion mechanism predicts parabolic reduction paths, and the paths obtained are asymptotic instead of parabolic. In addition the solid composition at which the reduction paths become asymptotic is a function of the operating variables. This result is not consistent with a simple diffusion model.

It is interesting to compare the effects of pressure (hence superficial gas velocity) at constant mass velocity for these runs at 1,300°F. (see Figure 5). For example at about 7 lb. moles/hr. sq.ft. the rate at 1.2 ft./sec is slightly faster than the rate at 1.5 ft./sec. The increased residence time of the gas as pressure increases (superficial gas velocity decreases) for this low mass velocity does not result in a significant increase in reduction rate because the gas in the bed is close to the equilibrium composition, particularly during the early stages of reduction. At about 12 lb. moles/hr. sq.ft. the rate is significantly faster at 1.2 ft./sec. than at 1.5 ft./sec. Finally at about 17 lb. moles/hr. sq.ft. the rate at 1.2 ft./sec. is much more rapid than at 1.5 ft./sec. Evidently when the pressure is increased at constant mass velocity, particularly for the higher mass velocities, the increased contact time of the gas results in an increased conversion, that is faster reduction. There is a dual nature to this phenomenon. It can be seen that the degree of reduction at which the paths become almost asymptotic increases with increasing pressure (increased gas residence time) for the same mass velocity, the effect being more pronounced as the mass velocity increases. At $G \sim 17$ lb. moles/hr. sq.ft. for example the asymptotic value for 5.4 atm. is about 93% reduction ($S = 0.10$), while the asymptotic value for 4.03 atm. is only 85% reduction ($S = 0.22$). Sintering and grain growth of the iron product layer are known to be time-dependent processes. Thus for the higher pressures, when the reduction is more rapid, much more chemical reaction can be accomplished before the competing physical processes of sintering and grain growth become effective in slowing down the reaction rate.

APPLICATION TO PROCESS DESIGN

Although the results of this study cannot be used directly for process design and evaluation, primarily because

scale-up phenomena are not well enough defined, they do provide useful qualitative guidance. It is evident that the batch-by-batch production of very highly reduced products should be done in two steps, a reduction to about 60% at 1,300°F. or higher and a final reduction at 1,000°F. or lower. In a continuous process on the other hand it has been shown (1) that final-bed operation at 1,300°F. produces a more highly reduced product (thus higher oxygen-removal rate) than a final bed operated at 1,000°F. An explanation of this apparently anomalous result is that the higher concentration of water vapor in the reducing gas during continuous operation retards the kinetics substantially at 1,000°F., whereas at the higher temperatures no such retardation is experienced.

Any process for moderately reduced products (70 to 80%) should be operated at a high temperature because the rate slowdown due to recrystallization is not severe below 80% reduction, at least for the higher mass velocities. This conclusion can be verified by comparing the reduction curves of Figure 3 with those of Figure 5. For example at a mass flow rate of about 17 lb. moles/hr. sq.ft. it required about 13 min. for the bed to reach 80% reduction ($S = 0.3$) at 1,000°F. compared with less than 9 min. at 1,300°F.

Obviously operation at higher pressures and gas mass velocities would result in increased productivity. However specifications of these variables are always dependent upon other factors, such as the particle-size distribution of the ore, the properties of construction materials for hydrogen preheaters, and the balance between the additional direct cost of the higher recycle ratio for higher pressures and gas mass velocities (lower conversion of reducing gas) and the indirect savings from the increased productivity of the plant.

NOTATION

- G = gas mass velocity, lb. moles/hr. sq.ft.
 K = equilibrium constant = $\left(\frac{P_{H_2O}}{P_{H_2}}\right)_{eq}$
 P = partial pressure, atm.
 $[Q/r_0 d_0]$ = rate function defined in reference 3
 S = atom ratio of oxygen to iron (O/Fe) in the particle (or bed)
 T = absolute temperature, °R.
 V = bed inventory, lb. moles Fe/sq.ft.
 y = mole fraction of water vapor in gas
 y_n = mole fraction inerts in gas
 θ = time, hr.
 π = total pressure, atm.

Subscripts

- o = initial condition and/or input condition
 θ = condition at time θ

LITERATURE CITED

1. Feinman, Jerome, I. & E. C. *Process Design and Development Quarterly*, 3, No. 3, pp. 241-247 (July, 1964).
2. Reed, T. F., J. C. Agarwal, and E. H. Shipley, *J. Metals*, 12, 317 (1960).
3. Feinman, Jerome, and T. D. Drexler, *A.I.Ch.E. Journal*, 7, No. 4, pp. 854-858 (1961).
4. McKewan, W. M., *Trans. Am. Inst. Mining Met. Engrs.*, 218, 545 (1960).
5. Humphrey, G. L., E. G. King, and K. K. Kelley, *United States Bureau of Mines Report of Investigations* 4870 (1952).
6. Darken, L. S., and R. W. Gurry, *J. Am. Chem. Soc.*, 67, 1398 (1945).

Manuscript received August 16, 1963; revision received February 10, 1964; paper accepted February 10, 1964. Paper presented at A.I.Ch.E. Houston meeting.